BREAKTHROUGH REPORT

Identifying root traits affecting root-substrate adhesion in Arabidopsis using a novel centrifugation technique

Bethany M Eldridge[1,*], Emily R Larson[1,*], Laura Weldon[1,a], Kevin M Smyth[1], Annabelle N Sellin[1], Isaac V Chenchiah[2], Tanniemola B Liverpool[2] and Claire S Grierson[1,#]

[1]School of Biological Sciences, University of Bristol, Bristol Life Sciences Building, 24 Tyndall Avenue, Bristol, BS8 1TQ, UK

[2]School of Mathematics, University of Bristol, Fry Building, Woodland Road, Bristol BS8 1UG, UK

[*]Authors contributed equally to this work.

[#]Corresponding author: lacsg@bristol.ac.uk

[a] Current address: Wildfowl and Wetlands Trust (WWT), Slimbridge, Gloucester, GL2 7BT, UK

ORCID:

BME: ORCID: 0000-0002-6598-3701

ERL: ORCID: 0000-0002-5498-8152

LW: ORCID: 0000-0002-0761-4414

KMS: ORCID: 0000-0003-0105-8557

IVC: ORCID: 0000-0002-8618-620X

TBL: ORCID: 0000-0003-4376-5604

CSG: ORCID: 0000-0002-4000-0975

Short title: Centrifuge assay quantifies root adhesion

One sentence summary: Using a novel centrifugation assay to identify root traits and novel genes that contribute to root-substrate adhesion in Arabidopsis.

The author responsible for distribution of materials integral to the findings presented in this article in accordance with the policy described in the Instructions for Authors (www.plantcell.org) is: Claire Grierson (lacsg@bristol.ac.uk).

ABSTRACT

The physical presence of roots and the compounds they release affect the cohesion between roots and their environments. However, we do not know the plant traits that are most important, which limits our ability to develop plant root systems with enhanced cohesion properties. Most methods that quantify the contributions particular traits make to substrate cohesion are time-intensive and require specialist equipment and complex substrates. We present an inexpensive, high-throughput phenotyping assay that can identify root traits and novel genes important for root-substrate adhesion by measuring the centrifugal force required to detach Arabidopsis seedlings from an agar medium. Using this method, we detected root hair shapes, vesicle trafficking pathways and root exudate composition that are important for root-substrate adhesion. We also used the assay to conduct a genetic screen, which identified an uncharacterised ABC transporter and demonstrates how this assay can be used to identify novel genes that affect root-substrate interactions.

INTRODUCTION

Plants secrete compounds that help them adapt to their environment, sense and interact with other organisms, and improve water and nutrient uptake (Bailey et al., 2002; Datta et al., 2011; Haling et al., 2013). These compounds, termed exudates, can vary in composition based on plant species, developmental stage, or environment (Naveed et al., 2017). Recent studies have shown that some compounds have bioadhesive properties that stick plants and soils together and aggregate soil particles, modifying the microenvironment around plant roots (Galloway et al., 2018).

Understanding how plant biology and physiology contribute to plant-soil interactions can be confounded by multiple factors: other organisms living in the soil also secrete organic metabolites that can contribute to soil cohesion, soil composition might affect plant exudate composition and vice versa. Also, plant root morphology including root architecture and root hairs can alter root-soil interactions (Baets et al., 2007; Bailey et al., 2002; Burylo et al.; Ghestem et al., 2014; Stokes et al., 2009). This complexity has made it difficult to characterise the relevant plant physiology.

Increasing centrifugal force has been used to measure the capacity of different tropical arboreal ant species to adhere to a smooth Perspex surface when spun at increasing speed in a centrifuge (Federle et al., 2000). We have developed a high-throughput assay that identifies and quantifies morphological and cellular contributions to root-substrate cohesion in a less variable environment than the natural rhizosphere. The assay uses a centrifuge to apply force to *Arabidopsis thaliana* seedlings grown on the surface of a sterile medium and measures the force required to detach seedlings from that surface. The adherence of candidate lines to the gel at increasing centrifugal force is then compared to a wild type control line. Applying a

Cox proportional hazards regression (Prentice and Kalbfleisch, 2003) to the results from centrifuging seedlings allows the adherence of candidate Arabidopsis lines relative to wild-type plants at increasing centrifugal force to be quantified.

Here, we show that our centrifugation method can be used to investigate how root hair morphology contributes to substrate adhesion and screen for biological components that do not present a visible phenotype. Using the genetic and molecular tools available in Arabidopsis and working in a sterile environment allows hypotheses about plant adhesive factors to be tested. While plant-soil cohesion is a complex and dynamic interaction, our assay provides a way to probe root cellular functions that might be masked by confounding variables in a soil-based study system. Results from this assay provide a platform for more comprehensive studies of plant morphology and physiology that promote root-substrate cohesion.

RESULTS

Experimental setup and aims

To measure the adhesion of Arabidopsis seedling roots using a centrifuge, it is important for roots to grow along the surface without penetrating the gel, and that seedlings do not touch each other, as both events could affect root-gel adhesion by interfering with seedling detachment during centrifugation. To prevent these issues from happening, ten seeds were sown 1 cm apart on a 90 mm Petri plate in two parallel rows**.** The plates were then orientated vertically at approximately 80° from horizontal and grown for 5-6 days in a growth chamber (Figure 1A). Individual plates and seedlings were visually evaluated to ensure that plants were at the same developmental stage and of similar size. Any seedlings that were touching each other, had grown into the gel, or not uniform in size were omitted from the assay. The seedlings were then numbered so that plate positional effects could be included as a potential covariate in the final analysis (Figure 1Bi). Plates were inverted and placed in centrifuge hanging baskets that held four plates at a time and subjected to increments of increasing centrifugal force at 720, 1018, 1247, 1440 and 1611 RPM for one minute each (Figure 1Bii), which applied centrifugal forces to the seedlings forty times gravity and above. The proportion of seedlings that detached from the gel surface was recorded between each centrifugal speed; a detachment event was recorded when a seedling had partially or fully peeled away from the gel (Figure 1Biii). If the gel shattered during the assay, seedlings that had not detached from the gel were not recorded. Seedlings that remained adhered to the gel

after the maximum centrifugal speed were censored in our analyses because we could not determine the centrifugal detachment force for those seedlings.

To calculate the centrifugal force acting on a seedling, the aerial tissue weight, angular velocity and the distance between the seedling and the axis of rotation in the centrifuge was used (Figure 1C and Equation 1). The aerial tissue weight of each seedling was measured because a plant with heavier aerial tissue experiences more force than a lighter one subjected to the same centrifugal speed.

A Cox proportional hazards (PH) regression model is a type of survival analysis used across different fields to study the timing of an event, such as the time for an animal to learn a behaviour, an individual to recover from a disease or die, or an electrical failure to occur (Allison, 2010; Miller, 1998). Here, the Cox proportional hazards (PH) regression model was used to statistically test for differences between the detachment of experimental seedlings relative to the wild-type control (Col-0) at increasing force. We used this regression model over other types of survival analyses because it is commonly used for testing whether covariates affect the time until an event occurs and can manage censored data (Devarajan and Ebrahimi, 2009). Seedling position and individual plate number were incorporated as covariates to account for any heterogeneity. In addition, because roots are developmentally plastic and sensitive to environmental heterogeneity (Bliss et al., 2002; Gao et al., 2004; Šmilauerová, 2001), we assessed the root-gel detachment of at least 70 plants from each line within a single experiment.

For each Cox PH regression model conducted, we evaluated (1) the P-value calculated from the Wald statistic (*z*-score) and (2) the hazard ratio with upper and lower bound confidence intervals. The hazard ratio is an exponential coefficient (Cox and Oakes, 1984) that was used to compare the risk of seedling detachment between candidate lines relative to wild type, and was used to measure effect size to assess differences between the root-gel adhesion of candidate lines and wild type. Wild type was used as the baseline group for all models, with a hazard ratio of one. A candidate line with higher risk of detachment from gel than wild type will have a hazard ratio above one. For example, a hazard ratio of 2.6 indicates that the line has 2.6 times the risk of seedling detachment from the gel compared to wild type. Conversely, lines with a lower risk of detachment than wild type will have a hazard ratio below one. For example, a hazard ratio of 0.4 indicates that the candidate line has a lower risk, only 0.4 times the detachment risk of wild type. A candidate line with a hazard ratio of 1.7 may also be interpreted as having a risk that has ***increased by*** 70% or is 0.7 times ***more*** relative to the hazard ratio of the wild-type control (Sedgwick, 2014).

While the centrifuge assay was initially optimized as one component of a report on how the absence or presence of root hairs affects root-substrate adhesion (De Baets et al., 2020), we wanted to test the capability of the assay to evaluate other traits and provide a highly quantifiable and affordable way to screen large populations of seedlings for the identification of new genetic factors important for plant-substrate interactions. To assess this, we used the assay to characterise: (1) mutants with different root hair morphologies to see if we could detect effects of root hair shape on adhesion; (2) mutants with altered vesicle trafficking but no known root hair morphological defects to identify trafficking functions that affect adhesion; (3) mutants with altered exudate composition but no known root hair morphological defects to detect effects of exudate composition; and (4) lines from a mutant population in a forward genetic screen to identify novel genes that affect root-substrate adhesion.

Root hair morphological effects on root-substrate adhesion

We screened mutant lines with known root hair morphology defects to ask if the centrifuge assay could determine if root hair shape affects root-substrate adhesion. The mostly bald mutant *csld3*, which encodes the CESA-like 3D protein (Favery et al., 2001; Yang et al., 2020) was included as a root hairless example. For lines that produce short or malformed root hairs, we included the *gdi1-2* Rho GTPase GDP dissociation inhibitor mutant, *rol1-2* rhamnose biosynthesis 1 mutant allele, *can of worms 1* (*cow1-3*) phosphatidylinositol transferase protein mutant, and *lrx1-4* leucine rich extensin 1 mutant (Baumberger et al., 2001; Böhme et al., 2004; Carol et al., 2005; Diet et al., 2006; Grierson et al., 1997). The *rol1-2* and *gdi1-2* mutants have short root hairs and the root hairs on *gdi1-2* plants can also branch (Parker et al., 2000; Ringli et al., 2008). *cow1-3* plants have short, wide root hairs that can branch, whilst *lrx1-4* plants can develop root hairs that abort, swell, branch, or collapse in a growth condition-dependent manner (Baumberger et al., 2001; Grierson et al., 1997; Parker et al., 2000). Under our growth conditions, we confirmed the reported phenotypes for each mutant line (Figure 2A).

Consistent with previous results (De Baets et al., 2020), bald (*csld3*) seedlings detached at lower centrifugal forces relative to wild-type seedlings, with 4.6 times the risk of detachment compared to wild-type plants (z = 8.644, P<0.001, HR = 4.636, 95% CI = 3.274 – 6.564; Figure 2B). Mutants with deformed root hair phenotypes including *gdi1-2*, *rol1-2*, *cow1-3* and *lrx1-4* had risks of detachment that were 2.5, 4, 3.8 and 3.9 times that of wild-type plants, respectively (*gdi1-2* – z = 5.199, P<0.001, HR = 2.459, 95% CI = 1.752 – 3.452;

175 *rol1-2* – *z* = 7.927, P<0.001, HR = 4.036, 95% CI = 2.858 – 5.698; *cow1-3* – *z* = 7.350,
176 P<0.001, HR = 3.790, 95% CI = 2.657 – 5.407; *lrx1-4* – *z* = 8.049, P<0.001, HR = 3.926,
177 95% CI = 2.814 – 5.478; Figure 2B-D). These results indicate that the centrifuge assay can
178 quantify effects of root hair shape on root-substrate cohesion. Many of the root hair mutants
179 tested are associated with changes in root hair cell wall composition, suggesting that
180 alterations in secreted compounds could affect root-substrate interactions in addition to any
181 physical or surface area-related factors that are specific to root hairs.
182
183 **Vesicle trafficking mutations affect root-substrate adhesion**
184 We hypothesized that Arabidopsis mutants with defective trafficking pathways
185 might alter cell wall and apoplast characteristics that contribute to root-substrate interactions
186 and adhesion. We chose the secretory Soluble NSF (N-ethylmaleimide sensitive fusion
187 protein) Attachment proteins (SNAP) REceptor (SNARE) mutants *syp121* and *syp122-1*, and
188 the endocytic mutants, *chc1-2* and *chc2-3* as candidates for our assay. SYP121 is the primary
189 secretory SNARE found on the plasma membrane (Assaad et al., 2004; Geelen et al., 2002)
190 and has characterized aboveground phenotypes, including small rosettes and stomatal
191 mobility defects (Eisenach et al., 2012; Larson et al., 2017); however, the mutant does not
192 have a reported root hair phenotype. Although the related SNARE SYP122 is thought to
193 share partial functionality with SYP121, the *syp122-1* mutant does not share these
194 phenotypes with *syp121* and a recent proteomic analysis reported differences in their vesicle
195 cargoes, which could contribute to their functional independence (Waghmare et al., 2018).
196 The *chc1-2* and *chc2-3* mutants are defective in the heavy chain subunits of the clathrin coat
197 complex, which is required for vesicle traffic at the plasma membrane (Kitakura et al., 2011).
198 Endo- and exocytic rates are impaired in both mutants (Larson et al., 2017), but no root hair
199 phenotypes have been reported. For the centrifuge assay, it was important to select mutants
200 that do not have root hair phenotypes given the effect root hair morphology has on root-gel
201 adhesion. Therefore, we evaluated the root hairs of these trafficking mutants and found that
202 the root hairs of these lines did not significantly differ from wild-type plants (Figure 3A).
203 Overall, the risk of detachment for *syp121*, *syp122-1*, *chc1-2* and *chc2-3* plants was
204 3.6, 3.3, 4.5 and 3.9 times that of wild type, respectively (*syp121* – *z* = 7.702, P<0.001, HR =
205 3.593, 95% CI = 2.595 – 4975; *syp122-1* – *z* = 7.199, P<0.001, HR = 3.270, 95% CI = 2.369
206 – 4.515; *chc1-2* – *z* = 8.238, P<0.001, HR = 4.482, 95% CI = 3.137 – 6.405; *chc2-3* – *z* =
207 7.653, P<0.001, HR = 3.941, 95% CI = 2.774 – 5.599; Figure 3B, C). Given that all the
208 mutants detached from the gel at lower centrifugal forces than wild-type seedlings, these

results indicate that the corresponding genes contribute to root-substrate adhesion and that the centrifuge assay can be used to probe for intracellular molecular machinery that affect root-substrate interactions.

Exudate composition changes root detachment rates

Over 20% of plant assimilated carbon is released as root exudates (Huang et al., 2016) that modify the external environment in response to abiotic and biotic stimuli and contribute to soil adhesion (Akhtar et al., 2018; Galloway et al., 2018). Root epidermal and hair cells secrete compounds that contribute to root exudate profiles that can be plant species specific (Naveed et al., 2017). Because mutants in both root hair development and vesicle trafficking pathways showed root-substrate adhesion phenotypes (Figures 2 and 3), we asked if the centrifuge assay could identify effects of exudate composition on root-substrate adhesion. We selected Arabidopsis mutants reported to have altered exudate composition compared to wild type, including *pft1-3*, *jin1-9*, and *pdr2* (Badri et al., 2009; Berger et al., 1996; Carvalhais et al., 2015; Kidd et al., 2009). *PFT1* (*MED25*) encodes the MEDIATOR25 subunit of the Mediator nuclear protein, and *JIN1* (*MYC2*) encodes a basic helix-loop-helix Leu zipper transcription factor; both proteins are involved in the jasmonate signalling pathway (Kidd et al., 2009; Lorenzo et al., 2004). *pft1-3* and *jin1-9* mutants are reported to have altered root exudate composition, including lower amounts of the amino acids asparagine, ornithine and tryptophan than wild-type plants (Carvalhais et al., 2015). *PDR2* (*ABCG30*) encodes a pleiotropic drug resistance (PDR) full-length ABC transporter that is involved in ABA transport and the exudation of secondary metabolites (Badri et al., 2008; Kang et al., 2015). We did not observe root hair growth phenotypes in these mutant lines compared to wild type (Figure 4A).

We found that compared to wild-type seedlings, *pdr2* seedlings resisted detachment, with 0.38 times the risk of detaching from the gel (z = -5.765, P<0.001, HR = 0.379, 95% CI = 0.273 – 0.528; Figure 4B). Conversely, *pft1-3* seedlings had an increased risk of detachment 1.7 times that of wild-type plants (z = 3.315, P<0.001, HR = 1.698, 95% CI = 1.242 – 2.323), and there was no difference in gel adhesion between *jin1-9* and wild-type plants (z = 0.737, P>0.05, HR = 1.124, 95% CI = 0.824 – 1.537; Figure 4B). These results show that exudate composition can alter root-substrate interactions, although this may not be the case for all exudate compositional changes, or identification of the effects of the exudate composition of the *jin1-9* mutant lay outside the sensitivity range of the assay. Since these mutant lines did not have root hair phenotypes, our results suggest that changes in exudate

243 composition alter root adhesive properties without affecting plant root hair morphology,
244 further indicating the power of the centrifuge assay as a potential mutant screening method.
245
246 **Centrifuge assay as a method for forward genetic screening**
247 Having demonstrated that our centrifugation technique can be used to identify
248 different types of traits that affect root-substrate adhesion, we conducted a forward genetic
249 screen to identify novel genes involved in root-substrate adhesion. To conduct this screen, the
250 root-gel adhesion properties of individual plants from a pooled SALK T-DNA insertion
251 mutant collection were analysed (Alonso et al., 2003). Individual plants with significantly
252 increased or decreased root-gel adhesion relative to wild-type plants were recovered from the
253 screen and self-fertilized to obtain progeny and identify the mutations. We identified a line
254 with significantly enhanced root-gel adhesion and conducted genomic Next-Generation
255 sequencing followed by Sanger sequencing of T-DNA flanking PCR products to confirm a T-
256 DNA insertion in the ABC transporter gene, *ABCG43,* whose function is unknown. We
257 named this T-DNA insertion line *abcg43*-1 and identified additional mutant alleles, *abcg43-2*
258 (SALK_201207c) and *abcg43-3* (SALKseq_30713) (Figure 5A).
259 We analysed the root-gel adhesion of homozygous insertional mutant alleles for
260 *ABCG43* and found *abcg43-1, abcg43*-2 *and abcg43*-3 plants resisted detachment from the
261 gel, with detachment risks 0.25, 0.35 and 0.2 times that of wild-type plants, respectively
262 (*abcg43-1* – z = -7.823, P<0.001, HR = 0.245, 95% CI = 0.172 – 0.348; *abcg43-2* – z = -
263 6.049, P<0.001, HR = 0.355, 95% CI = 0.253 – 0.496; *abcg43-3* – z = -7.179, P<0.001, HR =
264 0.203 – 0.403; Figure 5B, C). Collectively, these results suggest that disruption of *ABCG43*
265 expression and protein function affects root-gel adhesion. These results also illustrate the use
266 of the centrifuge assay as a powerful screening method for identifying novel genes involved
267 in root-substrate adhesion, as well as a tool for evaluating the effects of known gene function
268 on root-substrate interactions. Experiments are now being conducted to identify mutant
269 trait(s) in these lines and understand how *ABCG43* affects root-substrate adhesion.
270
271 **DISCUSSION**
272 To date, most published methods that quantify the contribution of particular traits to plant-
273 soil interactions are time-intensive, require specialist equipment and use complex substrates
274 (Bailey et al., 2002; De Baets and Poesen, 2010; De Baets et al., 2020; Toukura et al., 2006).
275 In contrast, our assay can produce data within a week, is available to any laboratory with
276 access to a bench top centrifuge and does not require speciality consumables. This method is

a high-throughput and quantitative way to test the effects of root morphology and cell function on root-substrate adhesion and to screen for new biological and molecular factors that can alter plant-substrate interactions. Using a defined model system like Arabidopsis and sterile medium conditions permits plant-specific characteristics to be identified that can then be probed in other substrate- or soil-based conditions.

Using the centrifuge assay to investigate the role of root hairs in root-substrate interactions

Results presented in this paper show that the centrifuge assay can quantify effects of root hair morphology on plant-substrate adhesion. By using well-characterized Arabidopsis root hair mutants, we demonstrate that this assay can evaluate the adhesive properties of mutants with a wide variety of root hair phenotypes. Previous work has shown that the presence of root hairs can significantly enhance root-substrate adhesion compared to the absence of root hairs (De Baets et al., 2020; Haling et al., 2013). Indeed, our centrifuge assay has previously been used to compare the forces required to detach seedlings with and without root hairs (De Baets et al., 2020); however, the sensitivity of the assay for comparing how root hair morphology affects root-substrate adhesion was not evaluated. We now show that this assay can distinguish the adherence strength of seedlings with altered root hair shapes and sizes (Figure 2), quantifying the contribution of these morphological traits to plant-substrate interactions. Some mutants with defective root hairs have mutations in cell wall biosynthesis and modification proteins, so it is possible that altered root-substrate interfaces compromise adhesion in these mutants, not just root hair shape. Using our method to rapidly phenotype mutants with root hair growth defects could direct additional experiments to characterize biochemical and morphological properties of genes of interest.

Identifying new genes involved in root-substrate adhesion

Mutations in cellular functions that do not alter root hair growth but do affect substrate adhesion can also be investigated using this assay. Vesicle trafficking pathways are required for cell wall deposition and maintenance (De Caroli et al., 2011; Larson et al., 2014; Rodriguez-Furlán et al., 2016); therefore, we hypothesized that mutants in trafficking pathways, particularly those at the plasma membrane, could affect root-substrate adhesion. Similarly, the composition and deposition of plant exudates help plants modify and optimize their growth conditions (Carvalhais et al., 2015; Naveed et al., 2017), suggesting that modification to plant exudate composition could affect root-substrate interactions. Consistent

with these hypotheses, mutants with vesicle trafficking defects and altered exudate composition have root-substrate adhesion properties that differ from wild type, indicating that this method can identify aspects of plant biology important for root-substrate interactions that do not affect root or root hair morphology (Figures 3 and 4). Our results further indicate that while root hairs provide significant adhesive and cohesive support both on solid gel and soil media (De Baets et al., 2020), there are additional cellular factors contributing to plant-substrate interactions that are not directly observable without the use of expensive antibodies, development of time-intensive transgenic lines, and microscopy equipment. Our centrifuge assay provides an affordable and quick alternative to these current methodologies.

We used this assay as a screen to identify new genes affecting plant-substrate interactions. As an example, we report the identification in a forward genetics screen of a mutant population in which *abcg43* mutant seedlings were more adhesive to gel than wild type. The function of ABCG43 in Arabidopsis is uncharacterised and therefore, this assay is a promising tool for identifying novel candidate genes that have no known association with root morphological defects, adhesion or exudate composition for future study.

CONCLUSION

This assay has applications in plant cell biology and genetics to understand how gene activity, cell function and root structure affect plant-soil adhesion and identify the molecular pathways involved. Potential applications include measuring variables not tested in this report, such as the effects of environmental conditions on plant-substrate adhesion and how other plant species or ecotypes respond to detachment forces. Given the recent discovery that root hair presence is important for Arabidopsis cohesion between roots and gel, and compost or soil (De Baets *et al.*, 2020), this assay could contribute to plant and soil sciences more broadly through the identification of plant traits that increase root-substrate cohesion and potentially stabilise slopes or reduce soil erosion.

METHODS

Plant material & growth conditions

Candidate lines of the Columbia-0 (Col-0) ecotype of *Arabidopsis thaliana* with T-DNA insertions or point mutations were obtained from the Nottingham Arabidopsis Stock Centre (NASC; Nottingham, UK) or were from stocks maintained in the lab (Table 1). Wild-type plants for all experiments were also the Col-0 ecotype. Homozygous lines of *csld3, cow1-3, lrx1-4, rol1-2, gdi1-2, chc1-2, chc2-3, syp121, syp122, jin1-9, pft1-3* and *pdr2* were

used in all experiments. Homozygosity of the *abcg43* mutant alleles was confirmed by genomic PCR analysis.

For all experiments, seeds were surface sterilised for 15 min in a solution containing 20% bleach and sterile water, followed by five washes in sterile water. All sterilised seeds were stratified in the dark at 4°C for 24-48 h in Eppendorf microtubes containing sterile water. All plants were reared in a growth room at 21-22°C with a continuous photoperiod (light intensity = 120-145 µmol m^{-2} s^{-1}) at 60% humidity.

For the centrifuge assay and morphological root trait analyses, sterile seeds were sown onto 90-mm Petri plates (Thermo Scientific RC2260). Ten seeds were sown in two rows of five on a single Petri plate containing 30 ml sterile gel medium and sealed with Parafilm (Bemis, NA**)**. The gel consisted of half strength Murashige and Skoog basal medium (Sigma M5519) with 1% [w/v] sucrose pH adjusted to 5.7, solidified with 1% [w/v] agar (Sigma A1296). Seed-sown plates were placed upright at ~80° from the horizontal (lid side down) to encourage vertical growth along the gel surface. Plants for genomic DNA extractions were grown in compost (three parts Levington F3 compost and one-part J Arthur Bowers horticultural silver sand).

Identification of *abcg43-1* mutant T-DNA insert

Genomic DNA was extracted from a pool of vegetative tissue taken from ten three-week old plants using an adapted protocol (Healey et al., 2014) for Illumina Next-Generation two x paired-end sequencing conducted at the Bristol Genomics Facility. The Illumina TruSeq Nano LT gDNA kit (Illumina Inc) was used to generate a genomic DNA sequencing library following the manufacturer's protocol. The final library was diluted to a loading concentration of 1.4 pM for cluster generation and 2 x 150 bp paired-end sequencing on the Illumina NextSeq500 system (Illumina Inc) alongside a 5% PhiX spike-in control library. Read summary statistics were generated using the RTA 2.4.6 Primary Analysis Software (Illumina Inc). The read summaries were analysed in the Sequencing Analysis Viewer (Illumina). Filtered paired reads were subject to paired-end alignment using the Bowtie2 2.3.4.2 aligner (Langmead and Salzberg, 2012). A bespoke reference genome was produced that combined the TAIR10 Arabidopsis genome (Lamesch et al., 2012) and the pROK2 vector sequence (Baulcombe et al., 1986). Alignments were viewed in the Integrative Genomics Viewer IGV 2.3 (Robinson et al., 2011).

For Sanger sequencing, DNA was extracted from a pool of vegetative tissue taken from two-week-old plants using a modified Edwards prep (Edwards et al., 1991). High

fidelity PCR was conducted on the *abcg43-1* line using the Q5 High-Fidelity 2X Master Mix (NEB). PCR products were purified and extracted from a 1% agarose gel using the QIAquick Gel Extraction Kit (QIAGEN), following the manufacturer's instructions. Purified PCR product plus the *abcg43-1* forward, reverse or border genotyping primer (Supplemental Table 1) was used for Sanger sequencing (using the Mix2Seq overnight sequencing kit, Eurofins Genomics). Chromatograms and FASTA files were obtained from Eurofin Genomics and following manual low-quality end trimming, the final sequences were aligned to the pROK2 vector sequence and *ABCG43* gene sequence using the MUSCLE alignment tool (Edgar, 2004).

Genotyping

To genotype the *abcg43* mutant alleles, genomic DNA was extracted from the vegetative tissue of two-week-old plants using a modified Edwards prep (Edwards et al., 1991). T-DNA border and gene-specific primers were used in PCR analyses to confirm the genotype (Supplemental Table 1).

Centrifuge assay set-up

After 5-6 days of growth, plates were placed in an inverted orientation into a hanging basket centrifuge (Beckman Allegra X-30R Centrifuge) and subjected to incremental increases of centrifugal force between 720 and 1611 RPM for one minute at a time; the proportion of seedlings that detached from the gel surface was recorded between each speed**.** The individual weight of aerial tissue for each seedling was measured using an analytical balance (Microbalance ME5; Sartorius). Centrifugal force, Fc (mN) acting on a seedling was calculated as previously reported in De Baets et al. (2020). Aerial tissue weight (kg), the angular velocity (ω) and the distance between the seedling and the axis of rotation on the centrifuge (radius = 0.07m) were used to give the following equation:

$$Fc = mass \times radius \times \omega^2 \qquad \text{(Equation 1)}$$

The root-gel detachment of at least 70 plants from each line was assessed within a single experiment. This replicate size was determined by preliminary experiments we conducted during assay development.

Morphological root trait analyses

Five-day-old Arabidopsis seedlings were imaged with a Leica MZ FLIII microscope (Leica) with dark-field lighting. Root hair length and density were measured using microscope images of five-day-old Arabidopsis seedlings and Fiji version 1.0 (Schindelin et al., 2012), using the Bio-Formats Importer plugin to load images into Fiji. At least two experimental repeats were conducted; in each experiment we imaged eight to ten individual plants from each line and measured at least 30 root hairs per plant.

Statistical analyses

All statistical analyses were conducted using RStudio, version 1.1453 (R Core Team, 2014) and all graphs were generated using the R package ggplot2 (Wickham, 2016).

For the centrifuge assay, we applied a Cox proportional hazards (PH) regression model to statistically test for differences between the rate of detachment of candidate lines relative to the wild type line (see results section). This analysis used the coxph function within the survival package in R and in all cases, the assumption of proportionality was satisfied. Comparisons of different candidate lines relative to the wild type line were analysed *a priori*; therefore, a series of contrasts were set up using the R function contr.treatment rather than using post-hoc testing methods. We censored seedlings that remained attached to the gel after the maximum centrifugal speed because we did not determine the speed these seedlings would have detached from the gel. Seedling position and the individual plate number were incorporated in the model as covariate factors; when these covariates had no significant effect, they were removed from the model. For each Cox PH regression model run, we report the P value of the Wald Statistic (*z*-score) and the hazard ratio with the upper and lower bound confidence intervals. A statistical level of 1% (0.01) was used.

To statistically test for differences between candidate lines relative to wild type plants for each of the root trait parameters measured, univariate analyses were conducted using the lm function in R. In all cases, the assumptions of normality and homoscedasticity were satisfied. Because comparisons of different mutant lines relative to the wild type line were set up *a priori*, a series of contrasts were set up using the contr.treatment function in R. To prevent type I errors from multiple testing, we applied the Bonferroni method and adjusted the alpha level to 0.025 (0.05/2).

SUPPLEMENTAL DATA

Supplemental Table 1. Genotyping primers used in this study

Supplemental Table 2. Centrifuge assay troubleshooting

ACKNOWLEGEMENTS

This work was supported by a Leverhulme Trust project grant RPG-2013-260 to CSG and TBL and BME was supported by a BBSRC SWBio PhD studentship (grant BB/M009122/1). We are thankful to Don Grierson FRS and Enrico Coen FRS who independently suggested the centrifuge assay concept, Timothy Quine for providing insightful guidance during method development, and Thomas Denbigh for providing essential technical advice. We are grateful to Jill Harrison, Victoria Spencer, Zoe Nemec Venza, Sophie Carpenter and Nicholas H Fair for their helpful comments during revision of the manuscript.

AUTHOR CONTRIBUTIONS

CSG designed the initial project, conducted proof-of-concept pilot experiments, obtained the funding, recruited the team and advised. TBL and IC developed the theoretical parametrisation of the centrifugal assay and bounds on the errors from other mechanical forces. BME and ERL planned and conducted all experiments apart from the genetic screen, which was carried out by LW and KMS. BME and ERL analysed all of the data presented herein. ANS and BME optimised the centrifuge assay data collection and data analysis methods. BME and ERL wrote the initial manuscript. BME, ERL, and CSG edited the manuscript. All authors reviewed and approved the final manuscript.

REFERENCES

Akhtar, J., Galloway, A.F., Nikolopoulos, G., Field, K.J., and Knox, P. (2018). A quantitative method for the high throughput screening for the soil adhesion properties of plant and microbial polysaccharides and exudates. Plant Soil *428*, 57–65.

Allison, P.D. (2010). Survival Analysis Using SAS: A Practical Guide, Second Edition (SAS Institute).

Alonso, J.M., Stepanova, A.N., Leisse, T.J., Kim, C.J., Chen, H., Shinn, P., Stevenson, D.K., Zimmerman, J., Barajas, P., Cheuk, R., et al. (2003). Genome-wide insertional mutagenesis of Arabidopsis thaliana. Science *301*, 653–657.

Assaad, F.F., Qiu, J.-L., Youngs, H., Ehrhardt, D., Zimmerli, L., Kalde, M., Wanner, G., Peck, S.C., Edwards, H., Ramonell, K., et al. (2004). The PEN1 Syntaxin Defines a Novel Cellular Compartment upon Fungal Attack and Is Required for the Timely Assembly of Papillae. Mol. Biol. Cell *15*, 5118–5129.

Badri, D.V., Loyola-Vargas, V.M., Broeckling, C.D., De-la-Peña, C., Jasinski, M., Santelia, D., Martinoia, E., Sumner, L.W., Banta, L.M., Stermitz, F., et al. (2008). Altered Profile of Secondary

Metabolites in the Root Exudates of Arabidopsis ATP-Binding Cassette Transporter Mutants. Plant Physiology *146*, 762–771.

Badri, D.V., Quintana, N., El Kassis, E.G., Kim, H.K., Choi, Y.H., Sugiyama, A., Verpoorte, R., Martinoia, E., Manter, D.K., and Vivanco, J.M. (2009). An ABC transporter mutation alters root exudation of phytochemicals that provoke an overhaul of natural soil microbiota. Plant Physiol. *151*, 2006–2017.

Baets, S.D., Poesen, J., Knapen, A., and Galindo, P. (2007). Impact of root architecture on the erosion-reducing potential of roots during concentrated flow. Earth Surface Processes and Landforms *32*, 1323–1345.

Bailey, P.H.J., Currey, J.D., and Fitter, A.H. (2002). The role of root system architecture and root hairs in promoting anchorage against uprooting forces in Allium cepa and root mutants of Arabidopsis thaliana. J. Exp. Bot. *53*, 333–340.

Baulcombe, D.C., Saunders, G.R., Bevan, M.W., Mayo, M.A., and Harrison, B.D. (1986). Expression of biologically active viral satellite RNA from the nuclear genome of transformed plants. Nature *321*, 446–449.

Baumberger, N., Ringli, C., and Keller, B. (2001). The chimeric leucine-rich repeat/extensin cell wall protein LRX1 is required for root hair morphogenesis in Arabidopsis thaliana. Genes Dev. *15*, 1128–1139.

Berger, S., Bell, E., and Mullet, J.E. (1996). Two Methyl Jasmonate-Insensitive Mutants Show Altered Expression of AtVsp in Response to Methyl Jasmonate and Wounding. Plant Physiology *111*, 525–531.

Bliss, K.M., Jones, R.H., Mitchell, R.J., and Mou, P.P. (2002). Are competitive interactions influenced by spatial nutrient heterogeneity and root foraging behavior? New Phytologist *154*, 409–417.

Böhme, K., Li, Y., Charlot, F., Grierson, C., Marrocco, K., Okada, K., Laloue, M., and Nogué, F. (2004). The Arabidopsis COW1 gene encodes a phosphatidylinositol transfer protein essential for root hair tip growth. Plant J. *40*, 686–698.

Burylo, M., Rey, F., Mathys, N., and Dutoit, T. Plant root traits affecting the resistance of soils to concentrated flow erosion. Earth Surface Processes and Landforms *37*, 1463–1470.

Carol, R.J., Takeda, S., Linstead, P., Durrant, M.C., Kakesova, H., Derbyshire, P., Drea, S., Zarsky, V., and Dolan, L. (2005). A RhoGDP dissociation inhibitor spatially regulates growth in root hair cells. Nature *438*, 1013–1016.

Carvalhais, L.C., Dennis, P.G., Badri, D.V., Kidd, B.N., Vivanco, J.M., and Schenk, P.M. (2015). Linking Jasmonic Acid Signaling, Root Exudates, and Rhizosphere Microbiomes. Mol. Plant Microbe Interact. *28*, 1049–1058.

Cox, D.R., and Oakes, D. (1984). Analysis of Survival Data (Boca Raton, Florida: Chapman & Hall/CRC Press).

Datta, S., kim, C.M., Pernas, M., Pires, N.D., Proust, H., Tam, T., Vijayakumar, P., and Dolan, L. (2011). Root hairs: development, growth and evolution at the plant-soil interface. Plant and Soil *346*, 1–14.

De Baets, S., and Poesen, J. (2010). Empirical models for predicting the erosion-reducing effects of plant roots during concentrated flow erosion. Geomorphology *118*, 425–432.

De Baets, S., Denbigh, T.D., Smyth, K.M., Eldridge, B.M., Weldon, L.M., Higgins, B.W., Matyjaszkiewicz, A.W., Meersmans, J., Larson, E.R., Chenchiah, I.V., et al. (2020). Micro-scale interactions between Arabidopsis root hairs and soil particles influence soil erosion. Nature Comms Biol *3*, 1–11.

De Caroli, M., Lenucci, M.S., Di Sansebastiano, G.-P., Dalessandro, G., De Lorenzo, G., and Piro, G. (2011). Dynamic protein trafficking to the cell wall. Plant Signal Behav *6*, 1012–1015.

Devarajan, K., and Ebrahimi, N. (2009). Testing for Covariate Effect in the Cox Proportional Hazards Regression Model. Commun Stat Theory Methods *38*, 2333–2347.

Diet, A., Link, B., Seifert, G.J., Schellenberg, B., Wagner, U., Pauly, M., Reiter, W.-D., and Ringli, C. (2006). The Arabidopsis root hair cell wall formation mutant lrx1 is suppressed by mutations in the RHM1 gene encoding a UDP-L-rhamnose synthase. Plant Cell *18*, 1630–1641.

Edwards, K., Johnstone, C., and Thompson, C. (1991). A simple and rapid method for the preparation of plant genomic DNA for PCR analysis. Nucleic Acids Res *19*, 1349.

Eisenach, C., Chen, Z.-H., Grefen, C., and Blatt, M.R. (2012). The trafficking protein SYP121 of Arabidopsis connects programmed stomatal closure and K^+ channel activity with vegetative growth. Plant J. *69*, 241–251.

Favery, B., Ryan, E., Foreman, J., Linstead, P., Boudonck, K., Steer, M., Shaw, P., and Dolan, L. (2001). KOJAK encodes a cellulose synthase-like protein required for root hair cell morphogenesis in Arabidopsis. Genes Dev. *15*, 79–89.

Federle, W., Rohrseitz, K., and Holldobler, B. (2000). Attachment forces of ants measured with a centrifuge: better 'wax-runners' have a poorer attachment to a smooth surface. Journal of Experimental Biology *203*, 505–512.

Galloway, A.F., Pedersen, M.J., Merry, B., Marcus, S.E., Blacker, J., Benning, L.G., Field, K.J., and Knox, J.P. (2018). Xyloglucan is released by plants and promotes soil particle aggregation. New Phytol. *217*, 1128–1136.

Gao, D., Knight, M.R., Trewavas, A.J., Sattelmacher, B., and Plieth, C. (2004). Self-reporting Arabidopsis expressing pH and [Ca2+] indicators unveil ion dynamics in the cytoplasm and in the apoplast under abiotic stress. Plant Physiol. *134*, 898–908.

Geelen, D., Leyman, B., Batoko, H., Di Sansebastiano, G.-P., Moore, I., Blatt, M.R., and Di Sansabastiano, G.-P. (2002). The abscisic acid-related SNARE homolog NtSyr1 contributes to secretion and growth: evidence from competition with its cytosolic domain. Plant Cell *14*, 387–406.

Ghestem, M., Cao, K., Ma, W., Rowe, N., Leclerc, R., Gadenne, C., and Stokes, A. (2014). A framework for identifying plant species to be used as "ecological engineers" for fixing soil on unstable slopes. PLoS ONE *9*, e95876.

Grierson, C.S., Roberts, K., Feldmann, K.A., and Dolan, L. (1997). The COW1 locus of arabidopsis acts after RHD2, and in parallel with RHD3 and TIP1, to determine the shape, rate of elongation, and number of root hairs produced from each site of hair formation. Plant Physiol *115*, 981–990.

562 Haling, R.E., Brown, L.K., Bengough, A.G., Young, I.M., Hallett, P.D., White, P.J., and George, T.S.
563 (2013). Root hairs improve root penetration, root-soil contact, and phosphorus acquisition in soils of
564 different strength. J. Exp. Bot. *64*, 3711–3721.

565 Healey, A., Furtado, A., Cooper, T., and Henry, R.J. (2014). Protocol: a simple method for extracting
566 next-generation sequencing quality genomic DNA from recalcitrant plant species. Plant Methods *10*,
567 21.

568 Huang, Y., Wang, Y., Tan, L., Sun, L., Petrosino, J., Cui, M.-Z., Hao, F., and Zhang, M. (2016).
569 Nanospherical arabinogalactan proteins are a key component of the high-strength adhesive secreted
570 by English ivy. Proc. Natl. Acad. Sci. U.S.A. *113*, E3193-3202.

571 Kang, J., Yim, S., Choi, H., Kim, A., Lee, K.P., Lopez-Molina, L., Martinoia, E., and Lee, Y. (2015).
572 Abscisic acid transporters cooperate to control seed germination. Nat Commun *6*, 8113.

573 Kidd, B.N., Edgar, C.I., Kumar, K.K., Aitken, E.A., Schenk, P.M., Manners, J.M., and Kazan, K.
574 (2009). The mediator complex subunit PFT1 is a key regulator of jasmonate-dependent defense in
575 Arabidopsis. Plant Cell *21*, 2237–2252.

576 Kitakura, S., Vanneste, S., Robert, S., Löfke, C., Teichmann, T., Tanaka, H., and Friml, J. (2011).
577 Clathrin mediates endocytosis and polar distribution of PIN auxin transporters in Arabidopsis. Plant
578 Cell *23*, 1920–1931.

579 Lamesch, P., Berardini, T.Z., Li, D., Swarbreck, D., Wilks, C., Sasidharan, R., Muller, R., Dreher, K.,
580 Alexander, D.L., Garcia-Hernandez, M., et al. (2012). The Arabidopsis Information Resource (TAIR):
581 improved gene annotation and new tools. Nucleic Acids Res. *40*, D1202-1210.

582 Langmead, B., and Salzberg, S.L. (2012). Fast gapped-read alignment with Bowtie 2. Nat Methods *9*,
583 357–359.

584 Larson, E.R., Domozych, D.S., and Tierney, M.L. (2014). SNARE VTI13 plays a unique role in
585 endosomal trafficking pathways associated with the vacuole and is essential for cell wall organization
586 and root hair growth in arabidopsis. Ann. Bot. *114*, 1147–1159.

587 Larson, E.R., Van Zelm, E., Roux, C., Marion-Poll, A., and Blatt, M.R. (2017). Clathrin Heavy Chain
588 Subunits Coordinate Endo- and Exocytic Traffic and Affect Stomatal Movement. Plant Physiol. *175*,
589 708–720.

590 Lorenzo, O., Chico, J.M., Sánchez-Serrano, J.J., and Solano, R. (2004). JASMONATE-
591 INSENSITIVE1 encodes a MYC transcription factor essential to discriminate between different
592 jasmonate-regulated defense responses in Arabidopsis. Plant Cell *16*, 1938–1950.

593 Miller, R.G. (1998). Survival Analysis (New York: Wiley & Sons).

594 Naveed, M., Brown, L.K., Raffan, A.C., George, T.S., Bengough, A.G., Roose, T., Sinclair, I.,
595 Koebernick, N., Cooper, L., Hackett, C.A., et al. (2017). Plant exudates may stabilize or weaken soil
596 depending on species, origin and time. European Journal of Soil Science *68*, 806–816.

597 Parker, J.S., Cavell, A.C., Dolan, L., Roberts, K., and Grierson, C.S. (2000). Genetic interactions
598 during root hair morphogenesis in Arabidopsis. Plant Cell *12*, 1961–1974.

599 Prentice, R.L., and Kalbfleisch, J.D. (2003). Mixed discrete and continuous Cox regression model.
600 Lifetime Data Anal *9*, 195–210.

R Core Team (2014). R: A language and environment for statistical computing (Vienna, Austria: R Foundation for Statistical Computing).

Ringli, C., Bigler, L., Kuhn, B.M., Leiber, R.-M., Diet, A., Santelia, D., Frey, B., Pollmann, S., and Klein, M. (2008). The Modified Flavonol Glycosylation Profile in the Arabidopsis rol1 Mutants Results in Alterations in Plant Growth and Cell Shape Formation. The Plant Cell *20*, 1470–1481.

Robinson, D.G., Scheuring, D., Naramoto, S., and Friml, J. (2011). ARF1 localizes to the golgi and the trans-golgi network. Plant Cell *23*, 846–849; author reply 849-850.

Rodriguez-Furlán, C., Salinas-Grenet, H., Sandoval, O., Recabarren, C., Arraño-Salinas, P., Soto-Alvear, S., Orellana, A., and Blanco-Herrera, F. (2016). The Root Hair Specific SYP123 Regulates the Localization of Cell Wall Components and Contributes to Rizhobacterial Priming of Induced Systemic Resistance. Front Plant Sci *7*, 1081.

Schindelin, J., Arganda-Carreras, I., Frise, E., Kaynig, V., Longair, M., Pietzsch, T., Preibisch, S., Rueden, C., Saalfeld, S., Schmid, B., et al. (2012). Fiji: an open-source platform for biological-image analysis. Nat. Methods *9*, 676–682.

Sedgwick, P. (2014). How to read a Kaplan-Meier survival plot. BMJ *349*, g5608.

Šmilauerová, M. (2001). Plant root response to heterogeneity of soil resources: Effects of nutrient patches, AM symbiosis, and species composition. Folia Geobot *36*, 337–351.

Stokes, A., Atger, C., Bengough, A.G., Fourcard, T., and Sidle, R.C. (2009). Desirable plant root traits for protecting natural and engineered slopes against landslides. Plant and Soil *324*, 1–30.

Toukura, Y., Devee, E., and Hongo, A. (2006). Uprooting and shearing resistances in the seedlings of four weedy species. Weed Biology and Management *6*, 35–43.

Waghmare, S., Lileikyte, E., Karnik, R., Goodman, J.K., Blatt, M.R., and Jones, A.M.E. (2018). SNAREs SYP121 and SYP122 Mediate the Secretion of Distinct Cargo Subsets. Plant Physiology *178*, 1679–1688.

Wickham, H. (2016). ggplot2: Elegant Graphics for Data Analysis (Springer).

Yang, J., Bak, G., Burgin, T., Barnes, W.J., Mayes, H.B., Peña, M.J., Urbanowicz, B.R., and Nielsen, E. (2020). Biochemical and Genetic Analysis Identify CSLD3 as a beta-1,4-Glucan Synthase That Functions during Plant Cell Wall Synthesis. Plant Cell *32*, 1749–1767.

Yi, K., Menand, B., Bell, E., and Dolan, L. (2010). A basic helix-loop-helix transcription factor controls cell growth and size in root hairs. Nat. Genet. *42*, 264–267.

633 **TABLE**

634 **Table 1** *Arabidopsis* mutant lines used in this study

Mutant type	***Mutant***	***AGI code***[a]	***Mutant line***	***Referenced in***
Root hair shape	*cow1-3*	At4g34580	SALK_0021245	Böhme *et al.* (2004)
	csld3-1	At3g03050	CS899	Favery *et al.* (2001)
	lrx1-4	At1g12040	SALK_057038	Kim *et al.* (2006)
	rol1-2	At1g78570	CS16373	Diet *et al.* (2006)
	gdi1-2	At3g07880	SALK_035400	Kang *et al.* (2017)
Vesicle trafficking	*chc1-2*	At3g11130	SALK_103252	Kitakura *et al.* (2011)
	chc2-3	At3g08530	SALK_151638	Bourdais *et al.* (2016)
	syp121	At3g11820	-	Assaad *et al.* (2004)
	syp122-1	At3g52400	SALK_008617	Assaad *et al.* (2004)
Root exudate composition	*jin1-9*	At1g32640	SALK_017005	Anderson *et al.* (2004)
	pdr2	At4g15230	SAIL_811_F08	Badri *et al.* (2008)
	pft1-3	At1g25540	SALK_059316	Kidd *et al.* (2009)
Unknown	*abcg43-1*	At4g15236	N75206[b]	This study
	abcg43-2	At4g15236	SALK_201207	This study
	abcg43-3	At4g15236	SALKseq_30713	This study

635 [a]AGI refers to the Arabidopsis Genome Initiative. [b] Refers to identification of the *abcg43-1*
636 line from a pooled set of 100 SALK T-DNA insertion lines (stock number N75206, Alonso *et*
637 *al*., 2003).

638

FIGURE LEGENDS

Figure 1. Centrifuge assay workflow.

(A) i. Ten seeds (highlighted in pink) are sown onto the surface of sterile, solid gel growth medium in a single Petri plate in two horizontal rows. ii. The plates are stacked in groups of five and orientated vertically at approximately 80° to encourage the roots to grow down the surface of the gel medium. Plates are grown in a growth chamber with constant light (120-145 μmol m^{-2} s^{-1}) conditions at 22°C and 60% relative humidity.

(B) After 5-6 days, i. seedlings are visually analysed and numbered. ii. Petri plates are placed into a swing-out-bucket centrifuge in an inverted orientation with their roots pointing inward (indicated by the purple arrows). iii. After seedlings have been subjected to a one-minute pulses of increasing centrifugal speeds, seedling detachment is recorded.

(C) i. The aerial tissue mass of each seedling is determined using ii. an analytical scale to iii. determine the root-gel adhesion properties of candidate lines are compared to wild-type to assess whether they have increased (e.g. line y) or decreased (e.g. line x) adhesion to the sterile gel.

Figure 2. Physical root hair properties contribute to root-substrate adhesion.

(A) Root hair phenotypes of 5-d-old wild-type (Col-0), *lrx 1-4*, *csld3-1*, *cow1-3*, *rol1-2*, and *gdi1-2* seedlings grown on gel medium and statistical comparisons of mean root hair density (number per mm length of root) and mean root hair length (mm) for each mutant line relative to wild type. White asterisks on the root hair images indicate the characteristic root hair bulging phenotype in the *lrx1-4* mutant and the short, branching root hair phenotype in *gdi1-2*. Scale bar = 0.5 mm. In the table, the mean ± standard error is given for root hair density and root hair length of wild type and each mutant as well as a mean comparison to wild type, which is listed in bold. “No difference” is stated when there was no statistically significant difference between wild type and a mutant line. The statistical output of each univariate linear model is given. Significance: ‘***’ = < 0.001, ‘**’ = < 0.01.

Survival curves displaying the proportion of seedlings that adhered to the gel at increasing centrifugal force for **(B)** 92 wild type (Col-0 – black); 81 *lrx1-4* (light green); 70 *csld3-1* (green); **(C)** 82 wild type (Col-0 - black); 83 *cow1-3* (green); and **(D)** 77 wild type (Col-0-black); 85 *rol1-2* (light green); and 86 *gdi1-2* (dark green). Circled red crosses on the survival curves represent seedlings that remained adhered to the gel after the maximum centrifugal speed (1611 RPM). The results shown are from a representative experiment for at least two

672 independent experiments showing a statistically significant difference in adhesion between
673 mutant lines relative to wild type (Cox PH regression; alpha = 0.001). A single experiment
674 included ≥ 70 biological replicates for each candidate line.
675
676 **Figure 3. Vesicle trafficking mechanisms that contribute to root-substrate adhesion**
677 **(A)** Root hair phenotypes of 5-d-old wild-type (Col-0), *syp121, syp122-1, chc1-2* and *chc2-3*
678 seedlings grown on a gel medium and statistical comparisons of mean root hair density
679 (number per mm length of root) and mean root hair length (mm) for each mutant line relative
680 to wild type. Scale bar = 0.5 mm. In the table, the mean ± standard error is given for the root
681 hair density and root hair length of wild type and each mutant as well as a mean comparison
682 to wild type, which is listed in bold. "No difference" is stated when there was no statistically
683 significant difference between wild type and a mutant line. The statistical output of each
684 univariate linear model is given.
685 Survival curves displaying the proportion of seedlings that adhered to the gel at increasing
686 centrifugal force for **(B)** 87 wild type (Col-0 – black); 91 *syp121* (turquoise); 83 *syp122-1*
687 (blue/grey); and **(C)** 83 wild type (Col-0 - black); 70 *chc1-2* (dark blue)*;* and 72 *chc2-3*
688 (medium blue). Red crosses circled on the survival curves represent seedlings that remained
689 adhered to the gel after the maximum centrifugal speed (1611 RPM). The results shown are
690 from a representative experiment for at least two independent experiments showing a
691 statistically significant difference in adhesion between all mutant lines relative to wild type
692 (Cox PH regression; alpha = 0.001). A single experiment included ≥ 70 biological replicates
693 for each candidate line.
694
695 **Figure 4. Exudate composition changes root-substrate adhesion properties**
696 **(A)** Root hair phenotypes of 5-d-old wild-type (Col-0), *jin1-9, pdr2* and *pft1-3* seedlings
697 grown on a gel medium and statistical comparisons of mean root hair density (number per
698 mm length of root) and mean root hair length (mm) for each mutant line relative to wild type.
699 Scale bar = 0.5 mm. In the table, the mean ± standard error is given for the root hair density
700 and root hair length of wild type and each mutant as well as a mean comparison to wild type,
701 which is listed in bold. "No difference" is stated when there was no statistically significant
702 difference between wild type and a mutant line. The statistical output of each univariate
703 linear model is given.
704 **(B)** Survival curves displaying the proportion of seedlings that adhered to the gel at
705 increasing centrifugal force for 80 wild type (Col-0 – black), 81 *jin1-9* (light pink), 80 *pdr2*

(light orange), and 81 *pft1-3* (dark orange). The results shown are from a representative experiment for at least two independent experiments showing a statistically significant difference in adhesion between mutant lines relative to wild type (Cox PH regression; alpha = 0.001), except for *jin1-9*. A single experiment included ≥ 70 biological replicates for each candidate line.

Figure 5. Using the centrifuge assay in a forward genetic screen to identify root-substrate adhesion mutants

(A) T-DNA insert locations in *ABCG43* for each *abcg43* mutant allele, with insertions indicated by orange arrowheads. The *ABCG43* gene is located on chromosome four at position Chr4: 8,969,677-8,702,727 and contains 23 exons (dark green) and 22 introns (white gaps). *abcg43-1* has a T-DNA insert in the exon10/intron10 boundary, *abcg43-2* (SALK_201207) has a T-DNA insert in exon 2 and *abcg43-3* (SALKseq_30713) has a T-DNA insert in exon 3.

(B) Genomic PCR confirming the homozygosity of each *abcg43* mutant for the respective T-DNA inserts. Lanes **1** and **2** were loaded with the gene-specific and T-DNA-border PCR products from *abcg43* mutant lines. Lanes **3** and **4** were loaded with the gene-specific and T-DNA-border PCR products from a wild type (Col-0) genomic DNA template. Lanes **5** and **6** were loaded with the water controls for the gene-specific and T-DNA-border PCR reactions, respectively. '**L'** indicates the 100-bp ladder. The expected product sizes for the gene-specific PCRs were ~350 nt, ~1025 nt and ~1090 nt; the T-DNA-border PCR product sizes were ~400 nt, ~550 nt and ~750 nt for *abcg43-1, abcg43-2* and *abcg43-3* alleles, respectively.

(C) Survival curves displaying the proportion of seedlings that adhered to the gel at increasing centrifugal force for 79 wild type (Col-0 – black), 70 *abcg43-1* (dark pink), 85 *abcg43-2* (purple), and 73 *abcg43-3* (light purple). Red crosses circled on the survival curves represent seedlings that remained adhered to the gel after the maximum centrifugal speed (1611 RPM). The results are from a representative experiment for at least two independent experiments showing a statistically significant difference in adhesion between the mutant lines relative to wild type (Cox PH regression; alpha = 0.001). A single experiment included ≥ 70 biological replicates for each candidate line.

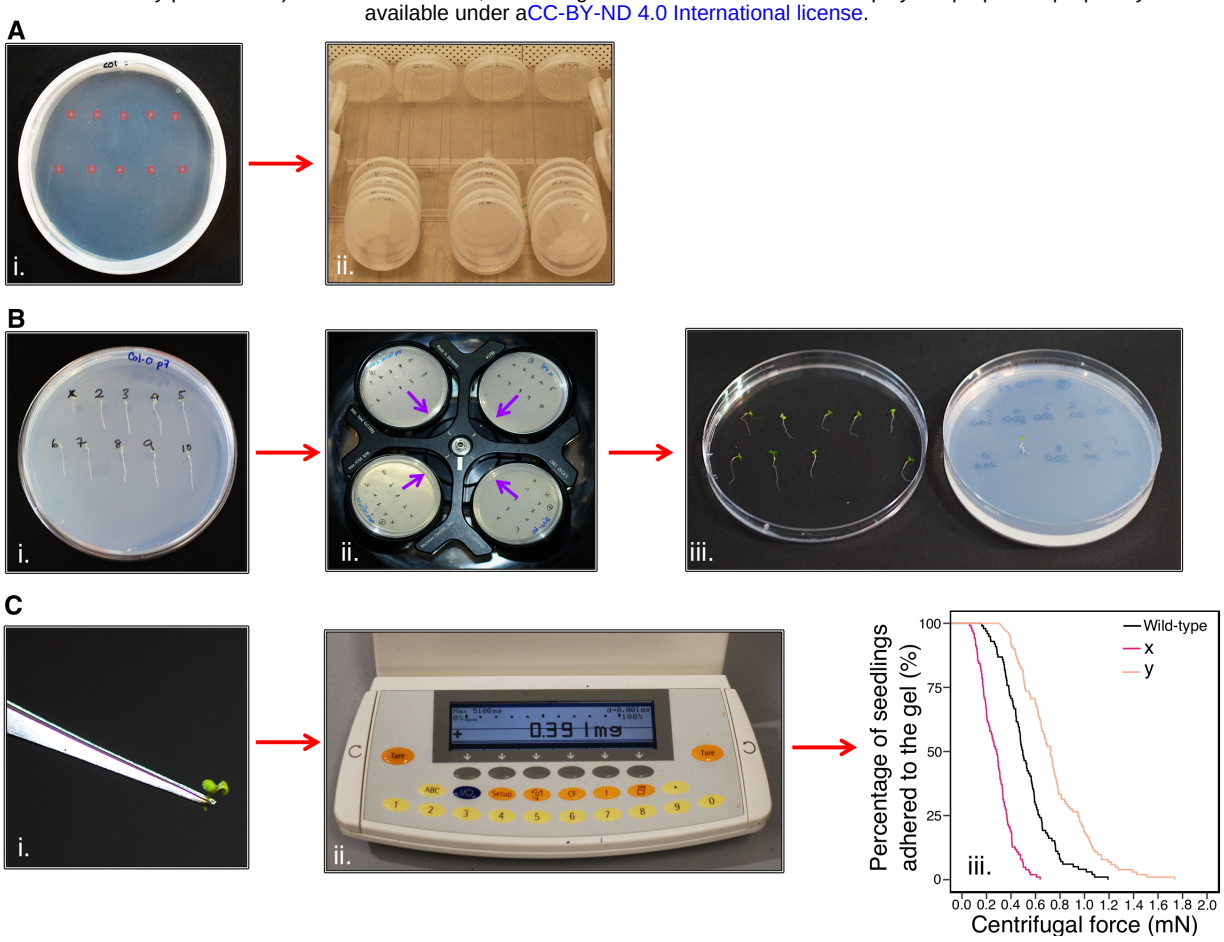

Figure 1. Centrifuge assay workflow.
(A) i. Ten seeds (highlighted in pink) are sown onto the surface of sterile, solid gel growth medium in a single Petri plate in two horizontal rows. ii. The plates are stacked in groups of five and orientated vertically at approximately 80° to encourage the roots to grow down the surface of the gel medium. Plates are grown in a growth chamber with constant light (120-145 µmol m^{-2} s^{-1}) conditions at 22°C and 60% relative humidity.
(B) After 5-6 days, i. seedlings are visually analysed and numbered. ii. Petri plates are placed into a swing-out-bucket centrifuge in an inverted orientation with their roots pointing inward (indicated by the purple arrows). iii. After seedlings have been subjected to a one-minute pulses of increasing centrifugal speeds, seedling detachment is recorded.
(C) i. The aerial tissue mass of each seedling is determined using ii. an analytical scale to iii. determine the root-gel adhesion properties of candidate lines are compared to wild-type to assess whether they have increased (e.g. line y) or decreased (e.g. line x) adhesion to the sterile gel.

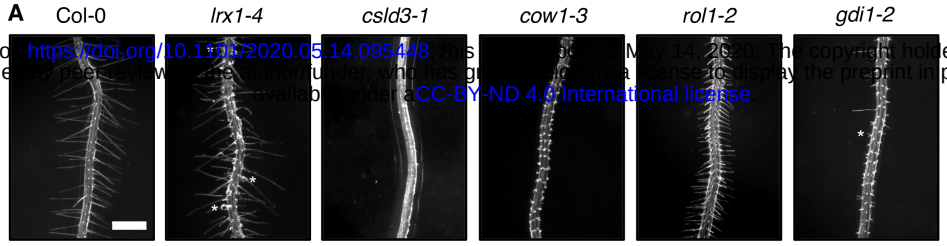

Line	Root hair density (number per mm length of root)		Root hair length (mm)	
Col-0	30.556 ± 0.784	-	0.518 ± 0.009	-
lrx1-4	31.889 ± 0.935 **No difference**	t = 1.093, P > 0.05 d.f. = 16, *n* = 9	0.388 ± 0.008 **1.3 times shorter****	t = -2.819, P < 0.001 d.f. = 16, *n* = 9
csld3-1	8.778 ± 1.188 **3.5 times less*****	t = -15.30, P < 0.001 d.f. = 16, *n* = 9	0.045 ± 0.002 **10.1 times shorter*****	t = -11.790, P < 0.001 d.f. = 16, *n* = 9
cow1-3	29.200 ± 0.772 **No difference**	t = -1.23, P > 0.05 d.f. = 17, *n* = 10	0.049 ± 0.001 **10 times shorter*****	t = -12.37, P < 0.001 d.f. = 17, *n* = 10
rol1-2	30.700 ± 1.550 **No difference**	t = 0.08, P > 0.05 d.f. = 17, *n* = 9	0.195 ± 0.003 **2.7 times shorter*****	t = -8.417, P < 0.001 d.f. = 17, *n* = 10
gdi1-2	26.200 ± 1.041 **0.17 times less****	t = -3.282, P < 0.01 d.f. = 17, *n* = 9	0.135 ± 0.006 **3.8 times shorter*****	t = -9.04, P < 0.001 d.f. = 16, *n* = 9

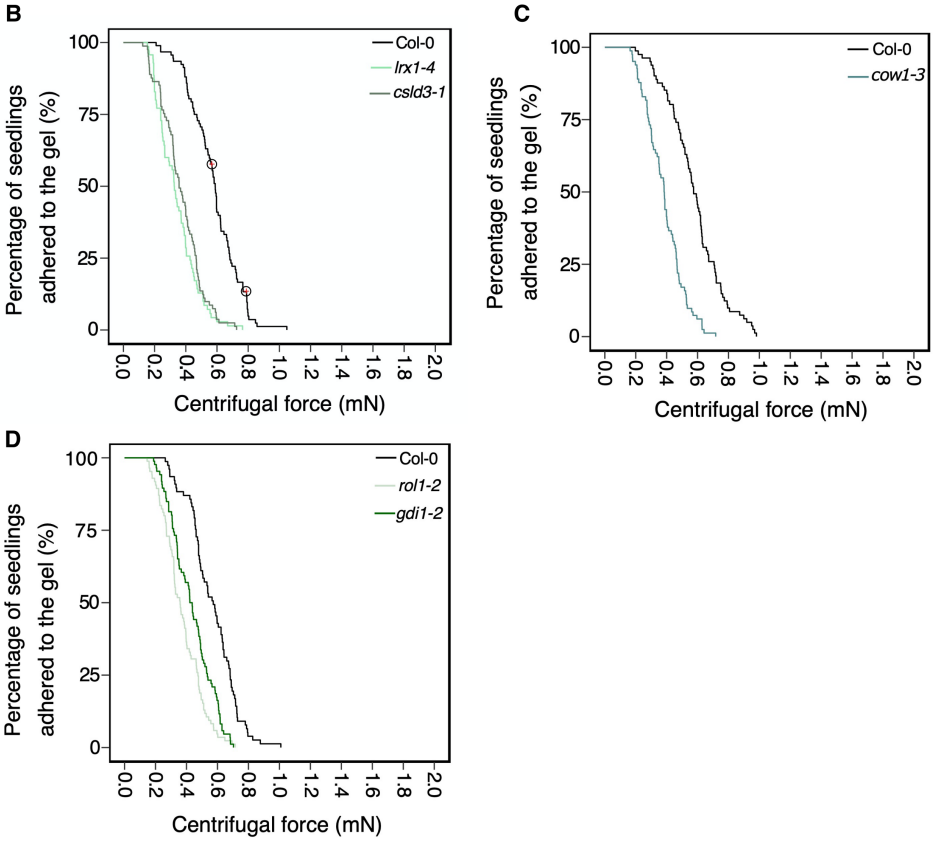

Figure 2. Physical root hair properties contribute to root-substrate adhesion.

(A) Root hair phenotypes of 5-d-old wild-type (Col-0), *lrx 1-4, csld3-1, cow1-3, rol1-2,* and *gdi1-2* seedlings grown on gel medium and statistical comparisons of mean root hair density (number per mm length of root) and mean root hair length (mm) for each mutant line relative to wild type. White asterisks on the root hair images indicate the characteristic root hair bulging phenotype in the *lrx1-4* mutant and the short, branching root hair phenotype in *gdi1*-2. Scale bar = 0.5 mm. In the table, the mean ± standard error is given for root hair density and root hair length of wild type and each mutant as well as a mean comparison to wild type, which is listed in bold. "No difference" is stated when there was no statistically significant difference between wild type and a mutant line. The statistical output of each univariate linear model is given. Significance: '***' = < 0.001, '**' = < 0.01.

Survival curves displaying the proportion of seedlings that adhered to the gel at increasing centrifugal force for **(B)** 92 wild type (Col-0 – black); 81 *lrx1-4* (light green); 70 *csld3-1* (green); **(C)** 82 wild type (Col-0 - black);

83 *cow1-3* (green); and **(D)** 77 wild type (Col-0- black); 85 *rol1-2* (light green); and 86 *gdi1-2* (dark green). Circled red crosses on the survival curves represent seedlings that remained adhered to the gel after the maximum centrifugal speed (1611 RPM). The results shown are from a representative experiment for at least two independent experiments showing a statistically significant difference in adhesion between mutant lines relative to wild type (Cox PH regression; alpha = 0.001). A single experiment included $\geq$ 70 biological replicates for each candidate line.

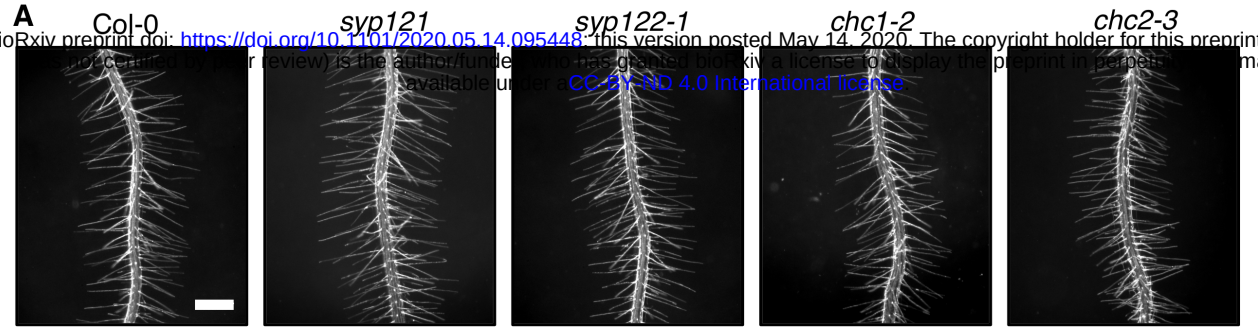

Line	Root hair density (number per mm length of root)		Root hair length (mm)	
Col-0	32.000 ± 0.632	-	0.420 ± 0.005	-
syp121	31.200 ± 0.952 **No difference**	t = -0.700, P > 0.05 d.f. = 18, *n* = 10	0.461 ± 0.004 **No difference**	t = 1.974, P > 0.05 d.f. = 18, *n* = 10
syp122-1	32.200 ± 0.442 **No difference**	t = 0.259, P > 0.05 d.f. = 18, *n* = 10	0.452 ± 0.005 **No difference**	t = 1.379, P > 0.05 d.f. = 18, *n* = 10
chc1-2	30.889 ± 0.716 **No difference**	t = -1.168, P > 0.05 d.f. = 17, *n* =9	0.441 ± 0.006 **No difference**	t = 0.684, P > 0.05 d.f. = 17, *n* = 9
chc2-3	31.889 ± 0.790 **No difference**	t = -0.111, P > 0.05 d.f. = 17, *n* = 9	0.463 ± 0.006 **No difference**	t = 0.182, P > 0.05 d.f. = 18, *n* = 10

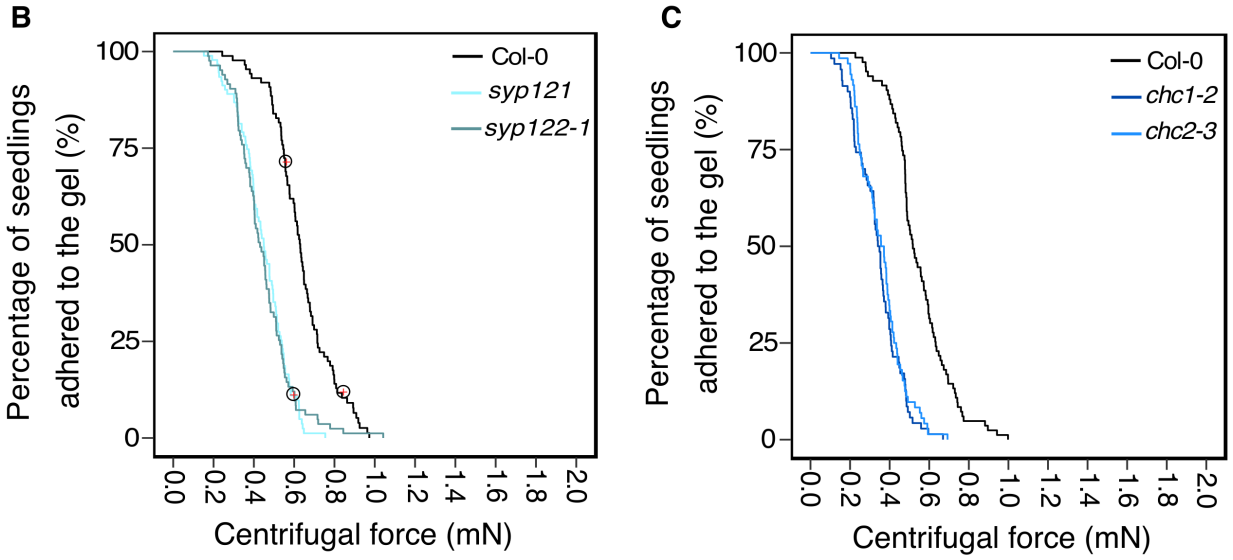

Figure 3. Vesicle trafficking mechanisms that contribute to root-substrate adhesion

(A) Root hair phenotypes of 5-d-old wild-type (Col-0), *syp121, syp122-1, chc1-2* and *chc2-3* seedlings grown on a gel medium and statistical comparisons of mean root hair density (number per mm length of root) and mean root hair length (mm) for each mutant line relative to wild type. Scale bar = 0.5 mm. In the table, the mean ± standard error is given for the root hair density and root hair length of wild type and each mutant as well as a mean comparison to wild type, which is listed in bold. "No difference" is stated when there was no statistically significant difference between wild type and a mutant line. The statistical output of each univariate linear model is given.

Survival curves displaying the proportion of seedlings that adhered to the gel at increasing centrifugal force for **(B)** 87 wild type (Col-0 – black); 91 *syp121* (turquoise); 83 *syp122-1* (blue/grey); and **(C)** 83 wild type (Col-0 - black); 70 *chc1-2* (dark blue)*;* and 72 *chc2-3* (medium blue). Red crosses circled on the survival curves represent seedlings that remained adhered to the gel after the maximum centrifugal speed (1611 RPM). The results shown are from a representative experiment for at least two independent experiments showing a statistically significant difference in adhesion between all mutant lines relative to wild type (Cox PH regression; alpha = 0.001). A single experiment included ≥ 70 biological replicates for each candidate line.

A

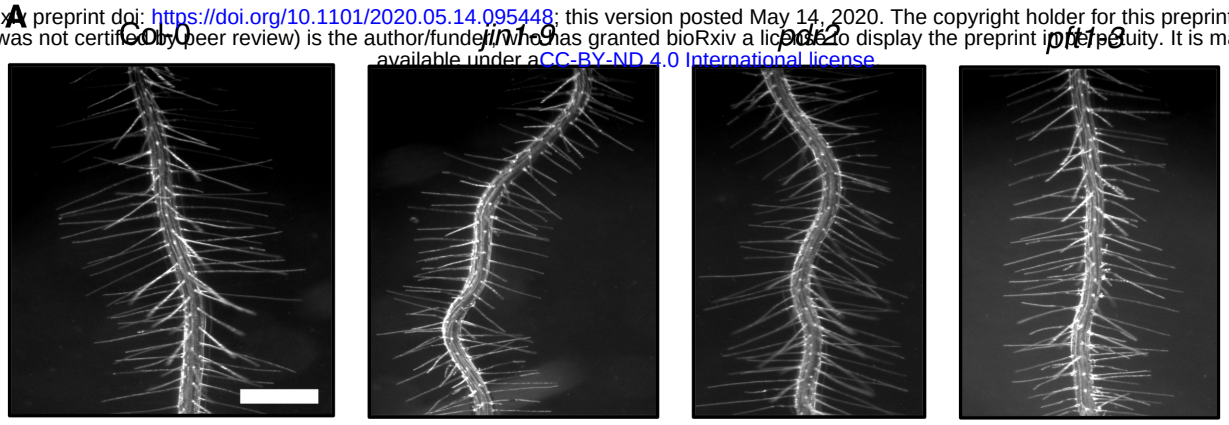

Line	Root hair density (number per mm length of root)		Root hair length (mm)	
Col-0	30.111 ± 1.612	-	0.416 ± 0.005	-
jin1-9	29.444 ± 1.271 **No difference**	t = -0.324, P > 0.05 d.f. = 16, *n* = 9	0.429 ± 0.006 **No difference**	t = 0.555, P > 0.05 d.f. = 16, *n* = 9
pdr2	31.125 ± 0.854 **No difference**	t = 0.533, P > 0.05 d.f. = 15, *n* =8	0.428 ± 0.006 **No difference**	t = 0.521, P > 0.05 d.f. = 15, *n* = 8
pft1-3	29.000 ± 1.179 **No difference**	t = -0.555, P > 0.05 d.f. = 16, *n* = 9	0.424 ± 0.006 **No difference**	t = 0.295, P > 0.05 d.f. = 16, *n* = 9

B

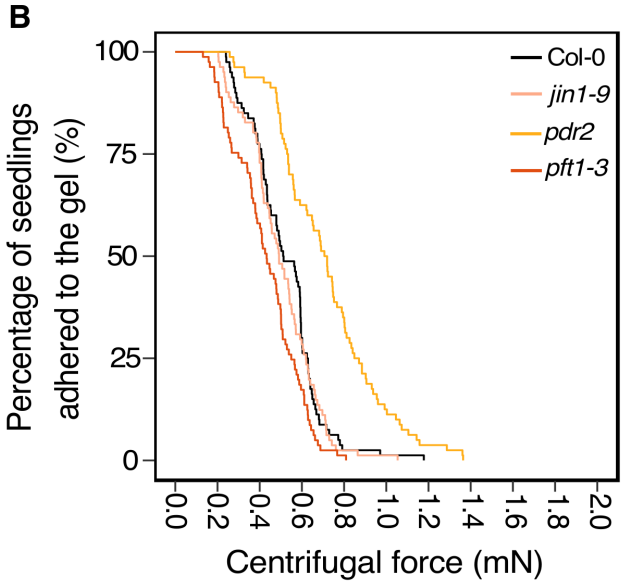

Figure 4. Exudate composition changes root-substrate adhesion properties

(A) Root hair phenotypes of 5-d-old wild-type (Col-0), *jin1-9, pdr2* and *pft1-3* seedlings grown on a gel medium and statistical comparisons of mean root hair density (number per mm length of root) and mean root hair length (mm) for each mutant line relative to wild type. Scale bar = 0.5 mm. In the table, the mean ± standard error is given for the root hair density and root hair length of wild type and each mutant as well as a mean comparison to wild type, which is listed in bold. "No difference" is stated when there was no statistically significant difference between wild type and a mutant line. The statistical output of each univariate linear model is given.

(B) Survival curves displaying the proportion of seedlings that adhered to the gel at increasing centrifugal force for 80 wild type (Col-0 – black), 81 *jin1-9* (light pink), 80 *pdr2* (light orange), and 81 *pft1-3* (dark orange). The results shown are from a representative experiment for at least two independent experiments showing a statistically significant difference in adhesion between mutant lines relative to wild type (Cox PH regression; alpha = 0.001), except for *jin1-9*. A single experiment included ≥ 70 biological replicates for each candidate line.

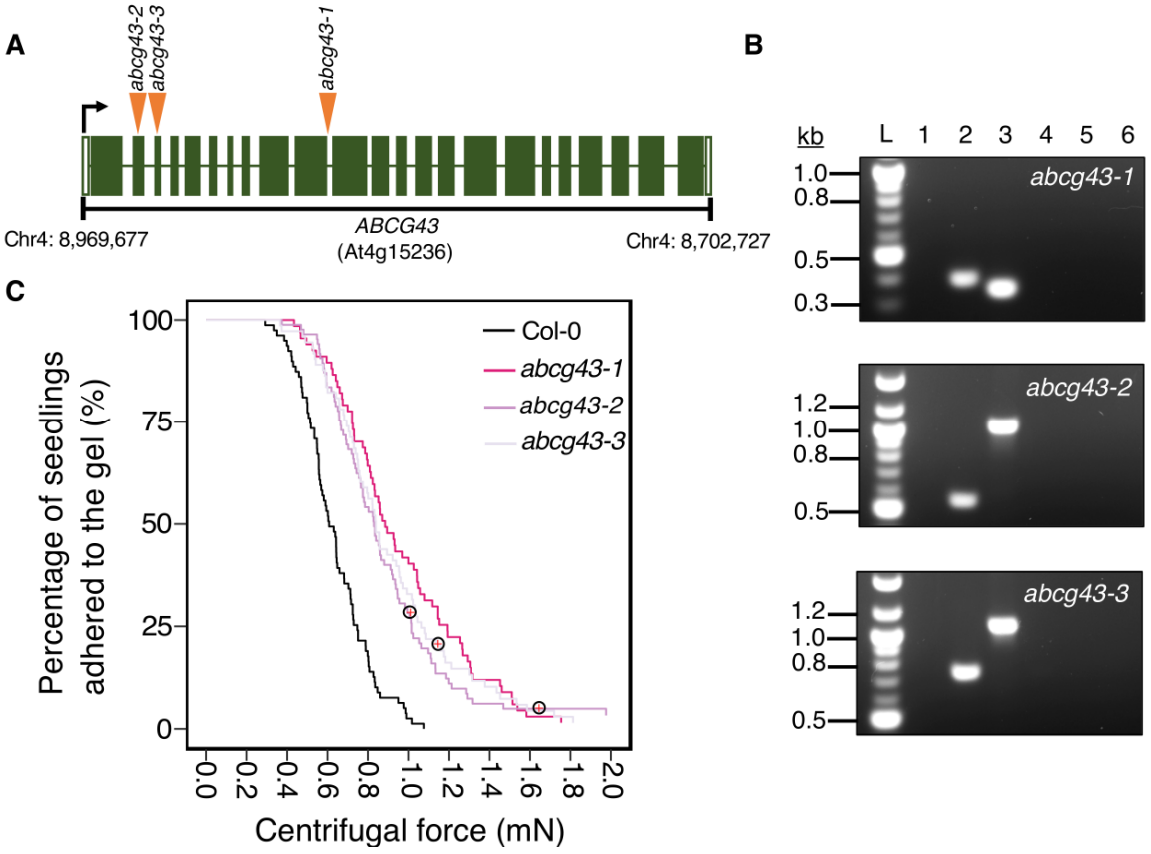

Figure 5. Using the centrifuge assay in a forward genetic screen to identify root-substrate adhesion mutants

(A) T-DNA insert locations in *ABCG43* for each *abcg43* mutant allele, with insertions indicated by orange arrowheads. The *ABCG43* gene is located on chromosome four at position Chr4: 8,969,677-8,702,727 and contains 23 exons (dark green) and 22 introns (white gaps). *abcg43-1* has a T-DNA insert in the exon10/intron10 boundary, *abcg43-2* (SALK_201207) has a T-DNA insert in exon 2 and *abcg43-3* (SALKseq_30713) has a T-DNA insert in exon 3.

(B) Genomic PCR confirming the homozygosity of each *abcg43* mutant for the respective T-DNA inserts. Lanes **1** and **2** were loaded with the gene-specific and T-DNA-border PCR products from *abcg43* mutant lines. Lanes **3** and **4** were loaded with the gene-specific and T-DNA-border PCR products from a wild type (Col-0) genomic DNA template. Lanes **5** and **6** were loaded with the water controls for the gene-specific and T-DNA-border PCR reactions, respectively. '**L**' indicates the 100-bp ladder. The expected product sizes for the gene-specific PCRs were ~350 nt, ~1025 nt and ~1090 nt; the T-DNA-border PCR product sizes were ~400 nt, ~550 nt and ~750 nt for *abcg43-1*, *abcg43-2* and *abcg43-3* alleles, respectively.

(C) Survival curves displaying the proportion of seedlings that adhered to the gel at increasing centrifugal force for 79 wild type (Col-0 – black), 70 *abcg43-1* (dark pink), 85 *abcg43-2* (purple), and 73 *abcg43-3* (light purple). Red crosses circled on the survival curves represent seedlings that remained adhered to the gel after the maximum centrifugal speed (1611 RPM). The results are from a representative experiment for at least two independent experiments showing a statistically significant difference in adhesion between the mutant lines relative to wild type (Cox PH regression; alpha = 0.001). A single experiment included $\geq$ 70 biological replicates for each candidate line.